Journal of Hand Surgery Global Online 3 (2021) 94–98

Contents lists available at ScienceDirect

Journal of Hand Surgery Global Online

journal homepage: www.JHSGO.org

Original Research

Prediction of Stress Distribution Applied to the Triangular Fibrocartilage Complex: A Finite Element Analysis

Takahiro Yamazaki, MD, * Yusuke Matsuura, PhD, * Akimoto Nimura, PhD, † Saya Horiuchi, MD, † Takane Suzuki, PhD, * Seiji Ohtori, PhD *

* Department of Orthopaedic Surgery, Graduate School of Medicine, Chiba University, Chiba, Japan
† Department of Functional Joint Anatomy, Graduate School of Medical and Dental Sciences, Tokyo Medical and Dental University, Tokyo, Japan

ARTICLE INFO

Article history:
Received for publication October 14, 2020
Accepted in revised form December 8, 2020
Available online January 16, 2021

Key words:
Biomechanical behavior
FEA
Schuind–Ekenstam paradox
Stress distribution
TFCC

Purpose: The triangular fibrocartilage complex (TFCC) is an important tissue stabilizer for the distal radioulnar joint, but stress distribution on the TFCC is not clear. The purpose of this study was to report the stress distribution of the TFCC using finite element analysis (FEA).
Methods: Pathological specimens of the wrist joint from an 80-year-old man were imported into a finite element analysis software package, and regions of interest including bone, soft tissue, and TFCC were extracted to create a 3-dimensional model. The material properties were obtained from previous research using cadaver specimens. To allow large deformations, we used hyperelastic elements to model the TFCC and soft tissue. Bone was defined as a uniform tissue that did not break. With the carpals and radius constrained, the rotation axis was set at the center of the ulnar head and a force was applied to move the ulnar head in pronation and supination. Under these boundary conditions, the behavior of the TFCC was extracted as a moving image. The average value of the maximum principal stress for each component of the TFCC was extracted and graphed.
Results: In the supinated position, the maximum principal stress was found on the palmar side of the TFCC (eg, on the tension side). In pronation, the maximum principal stress was found on the dorsal side.
Conclusions: This study clearly showed the 3-dimensional structure of the TFCC and analyzed its stress distribution under load. In supination, mean values of the maximum principal stress were greater on the palmar fibers than the dorsal fibers. In pronation, mean maximum principal stress was greater on the dorsal fibers than the palmar fibers.
Clinical relevance: Knowing the distribution of stresses in the TFCC is an important factor in developing treatment strategies for a pathologic TFCC.

Injury to the triangular fibrocartilage complex (TFCC) is a condition frequently encountered in daily practice as a cause of ulnar-sided wrist pain. This injury is broadly classified into traumatic and degenerative lesions.[1] Degenerative tears in the articular disk component of the TFCC are frequently attributed to ulnar impaction syndrome, which implies that excessive and chronic compressive loading across the ulnocarpal joint are the primary mechanical factors responsible for these tears.[2] In contrast, a tensile force caused by distraction of the distal radioulnar joint (DRUJ) has been implicated as an important mechanism for traumatic tears. Since Palmer and Werner's[2] report, there have been many reports on the anatomy and function of the TFCC. The TFCC is a compound structure composed of the articular disc, proximal and distal fibers, volar and dorsal radioulnar ligaments (RUL), ulnolunate ligament and ulnotriquetral ligaments, the ulnocollateral ligament, the sheath of the extensor carpi ulnaris tendon, the meniscus homologue, and the capsule.[2] The TFCC stabilizes the DRUJ by acting as a cushion for the ulnar head and lunate during axial loading and ulnar deviation of the wrist. It also limits ulnar deviation of the carpus.[2] There is still great debate about the function of the structures within the TFCC. For instance, it is not known which of the dorsal and volar fibers of the RUL are in tension with pronation or supination of the forearm (the Schuind–Ekenstam paradox).[3,4]

Declaration of interests: No benefits in any form have been received or will be received by the authors related directly or indirectly to the subject of this article.

Corresponding author: Takahiro Yamazaki, MD, Department of Orthopaedic Surgery, Graduate School of Medicine, Chiba University, 1-8-1 Inohana, Chuo-ku, Chiba 260-8670, Japan. (T. Yamazaki).
E-mail address: taka-0407@hotmail.co.jp (T. Yamazaki).

https://doi.org/10.1016/j.jhsg.2020.12.001

Nakamura and Makita[5] described the 3-dimensional structure of the TFCC as a hammock-like structure.

Finite element analysis (FEA) is a powerful tool for evaluating biomechanical behavior. Although it is impossible to visualize stress distribution inside the TFCC using a cadaver, FEA can be used to investigate stress distribution. Creating accurate models depends on knowing the material properties of the TFCC. A previous study measured the material properties of the TFCC using a fresh-frozen cadaver.[6]

The purposes of this study were to investigate the stress distribution of the TFCC using FEA analysis and to resolve the Schuind–Ekenstam paradox. We hypothesized that the palmar side would be tense during supination and the dorsal side would be tense during pronation.

Materials and Methods

Specimen

We obtained the wrist joint from an 80-year-old male cadaver.[7] We decalcified the wrist for 1 week in a solution containing aluminum chloride, hydrochloric acid, and formic acid, as described by Plank and Rychlo.[8] After decalcification, we dehydrated the block with a graded series of ethanols and embedded them in paraffin. The paraffin blocks were serially sectioned every 300 μm at a thickness of 5 μm/section parallel to the axial plane. The sections were stained with Masson trichrome.

Model creation

Tissue samples were converted to jpeg images. A model was created using an FEA software package (Mechanical Finder, Research Center for Computational Mechanics, Shinagawaku, Tokyo, Japan) from jpeg imaging data. Regions of interest of the ulna, radius, carpal, TFCC, and surrounding soft tissue were taken to create a model. The outer shape meshes were each 0.3 mm, the inner mesh was 2 mm at the maximum and 1 mm at the minimum, and the aspect ratio was 1.0. The material properties were homogeneous for bone, with a Young's modulus of 13.8 GPa and a Poisson's ratio of 0.3.[9] In the TFCC, based on the results of a previous study,[6] hyperelastic elements were used with Young's moduli for the palmar-side component of 5 MPa, the dorsal-side component of 6 MPa, the ulnar-side component of 9 MPa, the fovea fiber of 6 MPa, and the joint disk of 8 MPa. Based on these Young's moduli, the material constants of the Mooney–Rivlin model (C1 and C2) were calculated. Figure 1 shows the model created by this. For the sake of comparison with previous studies,[3,4,10] the palmar and dorsal radioulnar ligaments were divided into 2 layers, a superficial layer and a deep layer, at the center of the thickness (Fig. 2).

Boundary condition

For this model, pronation and supination were simulated by rotating the ulnar head. The radius and carpals were constrained, and the center of rotation was set at the fovea of the ulnar head (Fig. 3). Rotation was simulated by applying forces at 180° to both poles with respect to the center of rotation. In this model, a pronation of about 60° could be obtained by applying a force of 8 N, and a supination of about 60° could be obtained by applying a force of 10 N. Based on data from previous reports, [11–13] during pronation, the center of the ulnar head was forcibly displaced by 2.25 mm to the dorsal side. During supination, it was forcibly displaced by 1.35 mm to the palmar side.

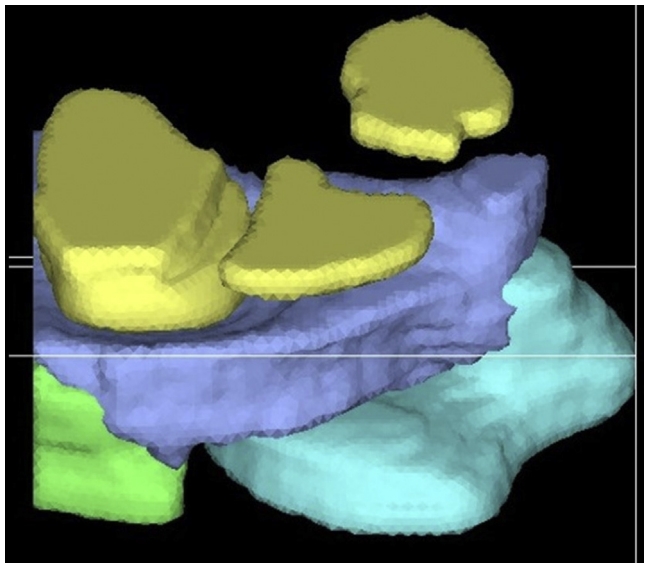

Figure 1. Three-dimensional model.

Evaluation

The behavior of the TFCC under these boundary conditions was extracted as a moving image. In addition, the average value of the maximum principal stress for each component of the TFCC (deep palmar fibers, superficial palmar fibers, deep dorsal fibers, and superficial dorsal fibers) was extracted and graphed.

Ethical approval

We obtained ethical approval for this study from the ethics committee (Judgment's Reference No. 3124).

Results

In supination, the mean values of maximum principal stress were greater in the order of deep palmar fibers followed by superficial palmar fibers, deep dorsal fibers, and then superficial dorsal fibers (Video 1, available on the *Journal's* Web site at www.jhsgo.org). The average values of maximum principal stress for each of these regions were 0.63, 0.37, 0.34, and 0.13 MPa, respectively, at maximum supination (60°) (Fig. 4).

In pronation, mean maximum principal stress was greater in the order of deep dorsal fibers followed by superficial dorsal fibers, superficial palmar fibers, and then deep palmar fibers (Video 2, available on the *Journal's* Web site at www.jhsgo.org). The average value of maximum principal stress for these regions was 1.09, 0.50, 0.19, and 0.01 MPa, respectively, at maximum pronation (60°) (Fig. 5).

Discussion

The results of this study differed from the Schuind–Ekenstam paradox. Similar to the report by Schuind et al,[4] in the current study, supination created a tensile stress on the palmar RUL, and the stress was greater in the deep layer than in the superficial layer. In addition, pronation created a tensile stress on the dorsal RUL, and the stress was greater in the deep layer than in the superficial layer.

Af Ekenstam and Hagert[3] suggested in 1985 that the deep fibers of the RUL were the main intrinsic stabilizers of the DRUJ. Those researchers used autopsy specimens and experimental techniques,

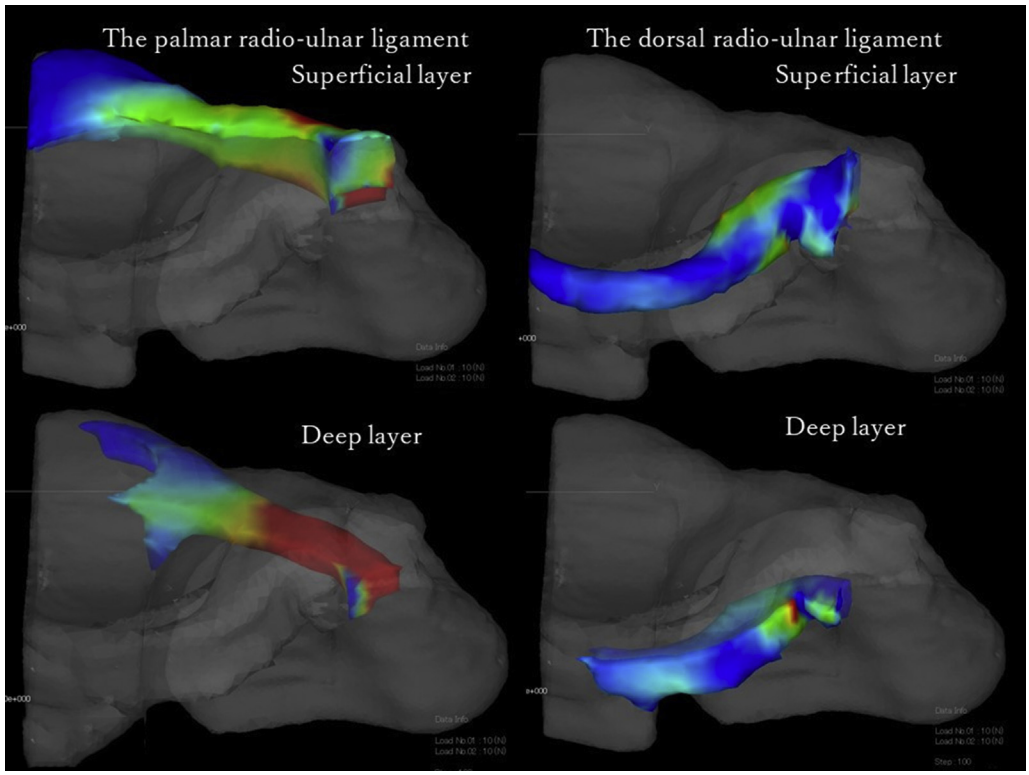

Figure 2. The palmar and dorsal radioulnar ligaments were divided into 2 layers, a superficial layer and a deep layer, at the center of the thickness.

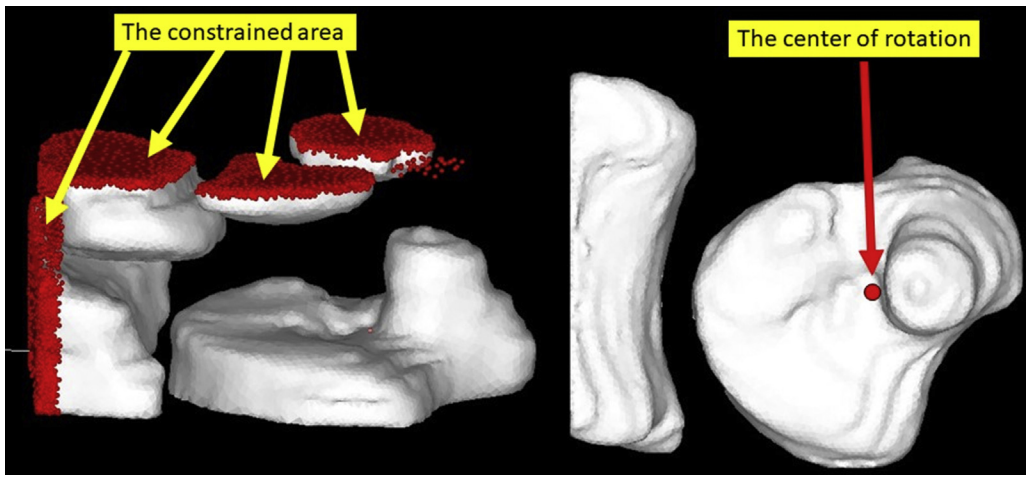

Figure 3. Boundary condition.

which may be considered basic by today's standards, but the conclusions were sound. In forearm supination, the deep fibers on the dorsal side of the RUL are notably tightened, whereas the deep palmar fibers remain loose. This suggests a pulling and tethering mechanism to control stability during DRUJ rotation.

In 1991, 6 years after the general consensus of the world of hand surgery,[3] based on that report of the main intrinsic stabilizers of forearm rotation, a breakthrough paper was published by Schuind et al[4] that proposed a completely different mechanism for forearm stability. Using sophisticated stereophotogrammetric techniques with phosphorescent markers and computer analysis, the authors concluded that the dorsal fibers of the RUL are tightened in pronation and the palmar fibers of the RUL are tightened in pronation.

In 1994, Hagert[10] revealed for the first time the biomechanical effects of each component of the TFCC. In this work, he inferred that his previous study evaluated only the deep components of the RUL inserted into the fovea of the ulna. This was the result of aggressive excision of the central articular disc in the 1985 study and affected the integrity of the dorsal and palmar superficial RUL. He also reported in the 1994 article that the phosphorescent marker that Schuind et al. applied to the surface of the RUL measured only developing tension or tightening of the superficial RUL, because these fibers enveloped the articular disc. However, the surface phosphorescent marker did not consider the biomechanics of the deep fibers of the RUL. In 1994, Hagert clarified that in forearm pronation, the superficial dorsal RUL must be tightened for stability,

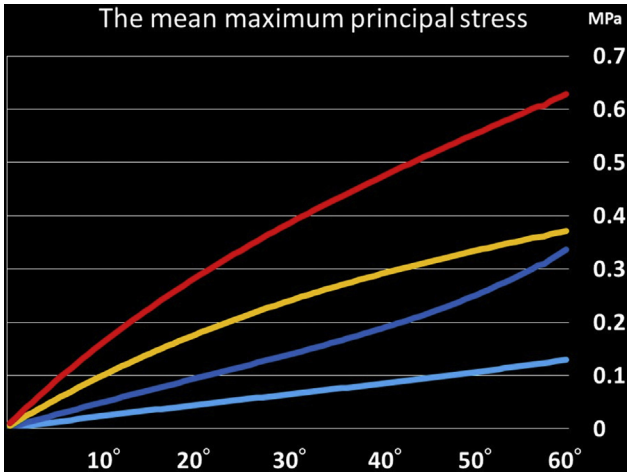

Figure 4. In supination: red line indicates deep palmar fibers; yellow, superficial palmar fibers; dark blue, deep dorsal fibers; and bright blue, superficial dorsal fibers.

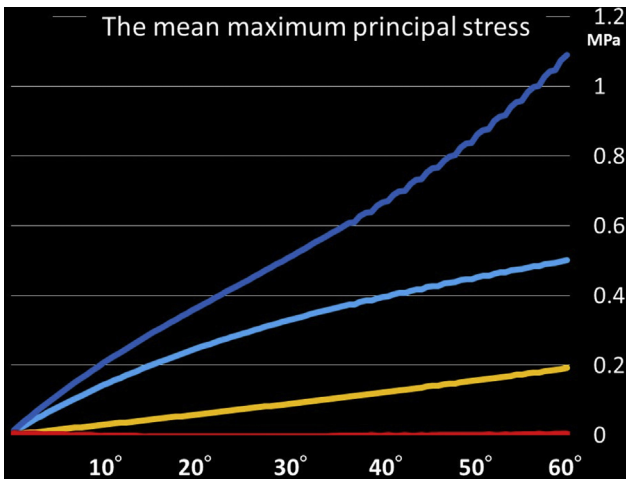

Figure 5. In pronation: dark blue line indicates deep dorsal fibers; bright blue, superficial dorsal fibers; yellow, superficial palmar fibers; and red, deep palmar fibers.

as is the deep palmar RUL. Conversely, in supination, both theories are correct because the superficial palmar RUL and the deep dorsal RUL are both tightened.

In this study, when a tensile force was applied to the palmar RUL in supination, the stress was greater in the deep layer than in the superficial layer. In addition, when a tensile force was applied to the dorsal RUL in pronation, the stress was greater in the deep layer than in the superficial layer.

The concept of the superficial and deep layers of the RUL is ambiguous. There are reports that the deep and superficial layers of the triangular fibrocartilage complex could not be clearly divided.[7,14] Therefore, superficial and deep layers were created for comparison with previous reports. For convenience, the thickness of the RUL was divided in half. The section mainly attached to the fovea was defined as the deep layer, and the section mainly attached to the ulnar styloid process was defined as the superficial layer.

In previous reports, the force applied to the RUL was examined in a state in which the 3-dimensional structure of the TFCC was lost by dissecting the DRUJ and removing the carpal. Therefore, different results came from the dissimilarities in the experimental approach and method of observation. In this study, the analysis was

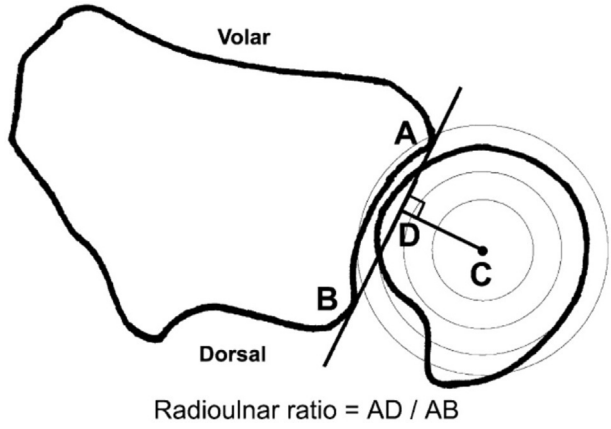

Figure 6. Radioulnar ratio.

performed while the 3-dimensional structure of the wrist including the carpals was maintained, and it was possible to perform the analysis in a more physiological environment. Our results show there is no difference in behavior between the deep and shallow layers as reported by Hagert et al.[10]

It is generally accepted that the ulnar head moves to the dorsal side relative to the radius in pronation and moves to the palmar side in supination. Park and Kim[11] measured the radioulnar ratio (Fig. 6) and reported it to be 0.66 in pronation, 0.51 in the neutral position, and 0.42 in supination. The AB distance in the current model is 15 mm, the AD distance is 9.9 mm in pronation, 7.65 mm in the neutral position, and 6.3 mm in supination. Therefore, it can be calculated that the ulnar head moves 1.35 mm to the palmar side when the forearm is supinated and 2.25 mm to the dorsal side when it is pronated. The total movement distance is 3.6 mm.

It is generally said that ulnar valiance (UV) increases with pronation,[15–17] but recent studies using computed tomography showed that UV hardly changed when the forearm was moved from pronation to supination.[12,13] Therefore, this study did not consider the change in UV during rotation. Moreover, the movement distance of the rotation center of the ulnar head was reported to be an average of 4.0 mm,[13] and the total movement distance of 3.6 mm is a reasonable value. The movement of the DRUJ during rotation in the current model reproduces past studies, validating the model.

This study had several limitations. First, the movement of the DRUJ may not have been completely reproduced. Normally, the radius moves around the ulna, but in this model the ulnar head is moved by restraining the radius. However, as described earlier, the ulna is displaced relative to its positional relation with the radius, which is close to the actual movement. Second, in this model, soft tissue is modeled by a hyperelastic element. Normal nonlinear analysis cannot withstand large deformation and breaks, so we could not perform an analysis without using hyperelastic elements. Third, this model is an isotropic model. The software, Mechanical Finder, cannot reflect anisotropy. Fourth, the tissue specimen used for modeling is an 80-year-old man, and the thickness and structure of the articular disc may be different from those of young people. In addition, the material properties are based on our previous studies, but these properties were defined from tissues taken from older people, so the model is applicable only to the elderly population. Fifth, this study validated just one specimen.

Acknowledgments

The authors wish to thank Mr Naoki Hara for advice on using Mechanical Finder.

References

1. Palmer AK. Triangular fibrocartilage complex lesions: a classification. *J Hand Surg Am*. 1989;14(4):594–606.
2. Palmer AK, Werner FW. The triangular fibrocartilage complex of the wrist-anatomy and function. *J Hand Surg Am*. 1981;6(2):153–162.
3. af Ekenstam F, Hagert CG. Anatomical studies on the geometry and stability of the distal radio ulnar joint. *Scand J Plast Reconstr Surg*. 1985;19(1):17–25.
4. Schuind F, An KN, Berglund L, et al. The distal radioulnar ligaments: a biomechanical study. *J Hand Surg Am*. 1991;16(6):1106–1114.
5. Nakamura T, Makita A. The proximal ligamentous component of the triangular fibrocartilage complex. *J Hand Surg Br*. 2000;25(5):479–486.
6. Yamazaki T, Matsuura Y, Suzuki T, Ohtori S. Measurement of the material properties of the triangular fibrocartilage complex. *J Hand Surg Glob Online*. 2020;2(2):90–93.
7. Horiuchi S, Nimura A, Tsutsumi M, et al. Anatomical relationship between the morphology of the styloid process of the ulna 2 and the attachment of the radioulnar ligaments. *J Anat*. 2020;237(6):1032–1039.
8. Plank J, Rychlo A. A method for quick decalcification. *Zentralbl Allg Pathol*. 1952;89(8):252–254.
9. Anderson DD, Deshpande BR, Daniel TE, Baratz ME. A three-dimensional finite element model of the radiocarpal joint: distal radius fracture step-off and stress transfer. *Iowa Orthop J*. 2005;25:108–117.
10. Hagert CG. Distal radius fracture and the distal radioulnar joint anatomical considerations. *Handchir Mikrochir Plast Chir*. 1994;26(1):22–26.
11. Park MJ, Kim JP. Reliability and normal values of various computed tomography methods for quantifying distal radioulnar joint translation. *J Bone Joint Surg Am*. 2008;90(1):145–153.
12. Kawanishi Y, Moritomo H, Omori S, Kataoka T, Murase T, Sugamoto K. A comparison of 3-D computed tomography versus 2-D radiography measurements of ulnar variance and ulnolunate distance during forearm rotation. *J Hand Surg Eur Vol*. 2014;39(5):526–532.
13. Shin SH, Lee YS, Choi KY, Kwak DS, Chung YG. During forearm rotation the three-dimensional ulnolunate distance is affected more by translation of the ulnar head than change in ulnar variance. *J Hand Surg Eur Vol*. 2019;44(5):517–523.
14. Nakamura T, Yabe Y. Histological anatomy of the triangular fibrocartilage complex of the human wrist. *Ann Anat*. 2000;182(6):567–572.
15. Palmer AK, Glisson RR, Werner FW. Ulnar variance determination. *J Hand Surg Am*. 1982;7(4):376–379.
16. Tomaino MM. The importance of the pronated grip X-ray view in evaluating ulnar variance. *J Hand Surg Am*. 2000;25(2):352–357.
17. Yeh GL, Beredjiklian PK, Katz MA, Steinberg DR, Bozentka DJ. Effects of forearm rotation on the clinical evaluation of ulnar variance. *J Hand Surg Am*. 2001;26(6):1042–1046.